ELSEVIER

Contents lists available at ScienceDirect

International Journal of Thermal Sciences

journal homepage: www.elsevier.com/locate/ijts



A moving finite line source model to simulate borehole heat exchangers with groundwater advection

Nelson Molina-Giraldo a,*, Philipp Blum b, Ke Zhu a, Peter Bayer c, Zhaohong Fang d

- ^a University of Tübingen, Center for Applied Geoscience (ZAG), Sigwartstrasse 10, 72076 Tübingen, Germany
- b Karlsruhe Institute of Technology (KIT), Institute for Applied Geosciences (AGW), Kaiserstraße 12, 76131 Karlsruhe, Germany
- ^c ETH Zürich, Engineering Geology, Sonneggstrasse 5, 8092 Zurich, Switzerland
- ^d Shandong Jianzhu University, Fengming Road, Lingang Development Zone, Jinan 250101, China

ARTICLE INFO

Article history: Received 31 January 2011 Received in revised form 13 June 2011 Accepted 18 June 2011 Available online 10 August 2011

Keywords: Ground source heat pump Analytical solution Borehole heat exchanger Finite length Line source

ABSTRACT

Available analytical models for the thermal analysis of ground source heat pumps (GSHPs) either neglect groundwater flow or axial effects. In the present study a new analytical approach which considers both effects is developed. Comparison with existing analytical solutions based on the finite and infinite line source theory is carried out. This study shows that in general the heat transfer at the borehole heat exchanger (BHE) is affected by groundwater flow and axial effects. The latter is even more important for long simulation times and short borehole lengths. At the borehole wall the influence of the axial effect is restricted to Peclet numbers lower than 10, assuming the BHE length as characteristic length. Moreover, the influence of groundwater flow is negligible for Peclet numbers lower than 1.2. As a result for Peclet numbers between 1.2 and 10 the combined effect of groundwater flow and axial effects has to be accounted for when evaluating the temperature response of a BHE at the borehole wall and thus the use of the moving finite line source model is required.

© 2011 Elsevier Masson SAS. All rights reserved.

1. Introduction

Ground source heat pump (GSHP) systems are one of the major technologies for shallow geothermal energy production in many countries [1,2]. Through their use, significant amounts of fossil fuels can be saved and thus additional CO2 emissions can be avoided [3,4]. GSHP systems are closed systems, in which a heat carrier fluid is circulated within a buried vertical or horizontal borehole heat exchanger (BHE). By slow and permanent circulation, exchange of heat with the surrounding underground is accomplished, which is utilized for space heating, air conditioning and hot water supply of both commercial and residential buildings. Vertical borehole configurations are often favored to horizontal collectors because of their smaller space requirements and because they are less influenced by seasonal temperature fluctuations from the surface. In this system, one or more vertical pipes are installed down to depths of around 50-150 m [5], depending on the prevailing geological conditions and the specific energy demand.

In order to estimate the heat transfer at the vertical BHE, different numerical [6–11] and analytical methods [12–21] as well

as combination of the latter have been proposed [15,22,23]. Analytical solutions are widely used because of their simplicity and speed in computation. Most of the analytical approaches for the thermal analysis of BHEs presume conduction-dominated systems (i.e. natural groundwater flow is not considered), and they are based on the infinite line source or cylindrical source theory [13,15]. They are in particular applied for the evaluation of short-term geothermal field experiments such as thermal response tests (TRT) which usually range from 12 to 60 h [24]. These models, however, are less adequate for long-term simulations when axial effects become relevant, usually after 1.6 year of operation depending on the hydrogeological and operational conditions [25]. The temperature response for an infinite line source model (without groundwater flow) cannot reach steady state conditions and the temperature anomaly will increase to infinity with operations the state of the st

In contrast, the temperature response converges to steady state conditions when accounting for a finite length of the borehole and hence axial effects are considered. Axial effects can be quantified as the differences between the results obtained by using finite and infinite line source methods. The axial heat conduction at the bottom of the borehole accelerates the heat exchange between heat carrier fluid and the surrounding underground, and thus has to be regarded for optimal borehole design. For a specific energy demand

^{*} Corresponding author. Tel.: +49 7071 2973172; fax: +49 7071 5059. E-mail address: nelson.molina-giraldo@uni-tuebingen.de (N. Molina-Giraldo).

Nomenclature		T_{o}	undisturbed initial temperature of the porous medium (°C)
а	thermal diffusivity (m²/s)	ΔT	temperature change (°C)
С	specific heat capacity (J/kg/K)	ν_{T}	effective heat transport velocity (m/s)
Fo	Fourier number	u_x	Darcy velocity (m/s)
Н	borehole length (m)	<i>x</i> , <i>y</i> , <i>z</i>	space coordinates (m)
K_0	modified Bessel function of second kind and order zero		
n	total porosity	Greek symbols	
Ре	Peclet number	λ	bulk thermal conductivity of porous medium (W/m/K)
Q	heat flow rate extraction or injection (J/s)	ho	density (kg/m³)
Q_1	energy extraction or injection (J)	φ	polar angle
$q_{ m L}$	heat flow rate per unit length of the borehole (W/m)	ϕ , τ , ψ	integration parameters
r	distance to the source (m)	Θ	dimensionless temperature
r'	radial coordinate (m)		
R, R', Z, Z' dimensionless coordinates		Subscripts	
t	time (s)	m	mean temperature around a circle
T	average temperature of the porous medium (°C)	S	aquifer material (solids), steady-state
		W	water

of a GSHP system, accounting for the axial effects can reduce the required length and numbers of boreholes. Marcotte et al. [26] showed for an example design problem that the calculated borehole length could be 15% shorter when axial effects are considered, which ultimately means a more cost-efficient system. Since under many circumstances the axial effects are of high relevance, apposite analytical solutions have been developed. Eskilson [15] proposed the finite line source model by summing up the effect of point sources of equal energy injection/extraction. This model was improved and used for the evaluation of long-term behavior of BHEs [18,27,28]. These analytical solutions account for the axial effects; however, they do not consider groundwater flow.

If groundwater flow is present, advective transport has to be considered, which means that heat is also transported by the moving water. Chiasson et al. [6], Wang et al. [29], Fan et al. [11] and Raymond et al. [30] evaluated the effects of groundwater flow on the heat transfer into the BHE. They concluded that groundwater flow enhances heat transfer between the BHE and the aquifer. In this case, shorter or less BHEs are needed for the same technical performance. Sutton et al. [17] and Diao et al. [14] presented an analytical solution considering groundwater advection. They both concluded that groundwater flow can change considerably the temperature distribution in the vicinity of the borehole. In these analytical solutions the borehole is considered as an infinite line heat source and therefore the axial effects are not taken into account in either study.

Hence, the aim of the present study is to develop an analytical solution which takes into account both aspects: groundwater flow and axial effects. It overcomes the limitations of previous analytical models especially for long-term simulation. The new analytical approach is verified with the finite element code FEFLOW version 6.0 [31]. This commercial software package was already used in several studies for simulating applications of shallow geothermal energy [e.g., 32,33]. The new analytical formulation is also compared to existing analytical methods in order to discuss the influence of axial effects and groundwater flow on the temperature development at the borehole wall and around the BHE.

2. Existing analytical approaches

The presence of groundwater flow in the underground and the influence of the actual length of the borehole are rarely taken into account when simulating heat transfer of GSHP systems. Therefore, conduction dominated systems are usually assumed and the

borehole is approximated as an infinite line source. Few studies, however, have incorporated the effect of groundwater flow (moving infinite line source model) [14,17] or the axial effect (standard finite line source model) [15,18] in thermal analysis of BHEs. In the following section, these analytical models are presented.

There are other processes that influence the temperature response of the BHE, and therefore should be accounted for in other analytical solutions. Bandos et al. [12], for instance, developed finite length analytical solutions including vertical temperature variations caused by geothermal gradient and temperature fluctuations at the surface. Man et al. [16] proposed a solid cylindrical source model which considers the radial dimension of the BHE. The latter is suitable for short boreholes or piles in which the diameter becomes important in comparison with the installation depth. These approaches, however, are not shown in the present study and the focus of the paper is oriented to the combined effect of groundwater flow and axial effects.

2.1. Standard finite line source model — (FLS)

Traditionally, heat transport in porous medium without groundwater flow is described by the heat conduction equation [13], which can be expressed as follows:

$$\rho c \frac{\partial T}{\partial t} - \nabla \cdot (\lambda \nabla T) = 0 \tag{1}$$

where T denotes the average temperature of the porous medium in which local thermal equilibrium is assumed [34], λ is the bulk thermal conductivity, and ρc is the volumetric heat capacity of the bulk porous medium. The latter can be computed as the weighted arithmetic mean of the solids of the aquifer $(\rho_s c_s)$ and water $(\rho_w c_w)$ [35]:

$$\rho c = n \rho_{\rm w} c_{\rm w} + (1 - n) \rho_{\rm s} c_{\rm s} \tag{2}$$

The solution of the partial differential equation of heat transport (eq. (1)) for a continuous point source in an infinite porous medium with a uniform initial temperature (T_0) is given by [13]:

$$\Delta T(x, y, z, t) = \frac{Q}{4\pi\lambda r} erfc \left[\frac{r}{\sqrt{4at}} \right]$$
 (3)

where ΔT is the temperature change in the underground $|T_0 - T|$, Q is the heat flow rate extracted/injected, a the thermal diffusivity

 $(a=\lambda/\rho c)$, and $r=\sqrt{x^2+y^2+(z-z')^2}$ is the distance to the source located on the *z*-axis at the coordinates (0, 0, z'). The FLS model is constructed by applying the method of images and summing up contributions of the point sources of equal energy injection/extraction [15,18,26,27]. As a result, constant temperature boundary conditions at the surface and downward vertical heat flow losses (axial effects) are accounted for. Applying the method of images [15,18] to equation (3) yields:

$$\Delta T_{\text{FLS}}(x, y, z, t) = \frac{q_{\text{L}}}{4\pi\lambda} \left[\int_{0}^{H} \frac{1}{r} \operatorname{erfc} \frac{r}{\sqrt{4at}} dz' - \int_{-H}^{0} \frac{1}{r} \operatorname{erfc} \frac{r}{\sqrt{4at}} dz' \right]$$
(4)

where H is the borehole length. For steady state conditions, equation (4) reduces to:

source with infinite length along the *z*-direction with a continuous heat flow rate per unit length of the borehole, $q_{\rm L}$. Although a BHE is composed of a buried pipe that commonly is surrounded by grouting material, approximation by a line source is commonly accepted in heat transport models of GSHP systems [14,15,17]. The underground is assumed to be homogeneous with respect to the thermal and hydraulic parameters. For steady state conditions equation (9) becomes:

$$\Delta T_{\text{MILSs}}(x, y) = \frac{q_{\text{L}}}{2\pi\lambda} \exp\left[\frac{v_{\text{T}}x}{2a}\right] K_0 \left[\frac{v_{\text{T}}\sqrt{x^2 + y^2}}{2a}\right]$$
(10)

in which K_0 is the modified Bessel function of the second kind of order zero. Introducing the dimensionless variable $Pe = v_T H/a$ (Peclet number), we can express equations (9) and (10) in dimensionless forms as follows:

$$\Delta T_{FLSs}(x,y,z) = \frac{q_L}{4\pi\lambda} \ln \left[\frac{H - z + \sqrt{r'^2 + (H - z)^2}}{H + z + \sqrt{r'^2 + (H + z)^2}} \frac{2z^2 + 2z\sqrt{r'^2 + z^2} + r'^2}{r'^2} \right]$$
 (5)

where $r'=\sqrt{x^2+y^2}$. Introducing the dimensionless temperature rise $\Theta=4\pi\lambda\Delta T/q_{\rm L}$, the dimensionless coordinates $R'=\sqrt{x^2+y^2}/H$, $R=\sqrt{R'^2+(Z-Z')^2}$, Z=z/H, and Z'=z'/H, and the Fourier number $Fo=at/H^2$, we can express equations (4) and (5) in dimensionless forms:

$$\Theta_{\text{FLS}}(R', Z, Fo) = \left[\int_{0}^{1} \frac{1}{R} \operatorname{erfc} \frac{R}{2\sqrt{Fo}} dZ' - \int_{-1}^{0} \frac{1}{R} \operatorname{erfc} \frac{R}{2\sqrt{Fo}} dZ' \right]$$
(6)

$$\Theta_{\text{FLSs}}(R',Z) = \ln \left[\frac{1 - Z + \sqrt{R'^2 + (1 - Z)^2}}{1 + Z + \sqrt{R'^2 + (1 + Z)^2}} \frac{2Z^2 + 2Z\sqrt{R'^2 + Z^2} + R'^2}{R'^2} \right]$$
(7)

2.2. Moving infinite line source model — (MILS)

Heat transport in the porous media with groundwater flow is mainly accomplished by conduction through the fluid and solid phase and advection through the flowing water. The partial differential equation for advective and conductive heat transport in porous media can be expressed in a 2D form (x-y) plane as follows [36]:

$$\rho c \frac{\partial T}{\partial t} + u_{x} \rho_{w} c_{w} \frac{\partial T}{\partial x} - \lambda \left(\frac{\partial^{2} T}{\partial x^{2}} + \frac{\partial^{2} T}{\partial y^{2}} \right) = 0$$
 (8)

where u_x denotes an uniform Darcy velocity in the x-direction. The solution of equation (8) for an infinite porous medium with a uniform initial temperature is given by Sutton et al. [17] and Diao et al. [14]:

$$\Delta T_{\text{MILS}}(x, y, t) = \frac{q_{\text{L}}}{4\pi\lambda} \exp\left[\frac{v_{\text{T}}x}{2a}\right] \int_{0}^{v_{\text{T}}^2t/4a} \frac{1}{\psi} \exp\left[-\psi - \frac{v_{\text{T}}^2(x^2 + y^2)}{16a^2\psi}\right] d\psi$$
(9)

in which $v_T = u_x \rho_w c_w/\rho c$ is the effective heat transport velocity. This analytical solution applies for the response of a constant line

$$\Theta_{\rm MILS}(R', \varphi, Fo, Pe) = \exp\left[\frac{Pe}{2}R'\cos(\varphi)\right] \\ \times \int_{2}^{Pe^{2}Fo/4} \frac{1}{\psi}\exp\left[-\psi - \frac{Pe^{2}R'^{2}}{16\psi}\right] d\psi \qquad (11)$$

$$\Theta_{\text{MILSs}}(R', \varphi, Pe) = 2\exp\left[\frac{Pe}{2}R'\cos(\varphi)\right]K_0\left[\frac{Pe}{2}R'\right]$$
 (12)

Groundwater flow velocities are highly variable depending on the hydrogeological conditions. This variability is especially attributed to the hydraulic conductivity which can range over more than 8 orders of magnitude [37]. For instance, the hydraulic conductivity of sandy sediments can vary from 10^{-5} m/s to 10^{-3} m/s. Assuming a constant and typical hydraulic gradient of 10^{-3} , the Darcy velocity ranges from 10^{-8} m/s to 10^{-6} m/s for fine and coarse sands, respectively.

3. Moving finite line source model-(MFLS). New approach

For long-term period simulations, axial effects become more evident when simulating heat transfer at the BHE [16]. Existing analytical solutions that account for axial effects still do not consider groundwater flow. Hence, the new analytical approach proposed here takes into account both effects, while the following assumptions are made:

- a) The underground is considered as a homogeneous semiinfinite porous medium, which is initially at thermal equilibrium and its thermal properties are independent of the temperature changes.
- b) The boundary of the ground surface has a fixed temperature equal to the initial temperature of the underground and natural geothermal gradient is not accounted for.
- c) A constant heat flow rate per unit length of the borehole (q_L) is applied to a line source of finite length, which stretches along the z-axis down to a certain depth H.

The starting point for the finite line source model is the Green's function of an instantaneous point source (eq. (A1)). The moving

finite line source model is obtained by applying the method of images [15] and the moving source theory [13] to equation (A1). The detailed derivation is presented in the Appendix.

The transient solution reads:

$$\Delta T_{\text{MFLS}}(x,y,z,t) = \frac{q_{\text{L}}}{2\pi\lambda} \exp\left[\frac{\nu_{\text{T}}x}{2a}\right] \times \left[\int_{0}^{H} f(x,y,z,t) \, \mathrm{d}z' - \int_{-H}^{0} f(x,y,z,t) \, \mathrm{d}z'\right]$$
(13)

$$f(x,y,z,t) = \frac{1}{4r} \left[\exp\left(-\frac{v_{T}r}{2a}\right) erfc\left(\frac{r - v_{T}t}{2\sqrt{at}}\right) + \exp\left(\frac{v_{T}r}{2a}\right) erfc\left(\frac{r + v_{T}t}{2\sqrt{at}}\right) \right]$$
(14)

As time approaches infinity, the steady state solution is derived as follows:

$$\Delta T_{\text{MFLSs}}(x, y, z) = \frac{q_{\text{L}}}{4\pi\lambda} \exp\left[\frac{v_{\text{T}}x}{2a}\right] \left[\int_{0}^{H} \frac{1}{r} \exp\left[-\frac{v_{\text{T}}r}{2a}\right] dz'\right] - \int_{-H}^{0} \frac{1}{r} \exp\left[-\frac{v_{\text{T}}r}{2a}\right] dz'$$
(15)

In order to keep the number of independent variables to the minimum, equations (13)–(15) can be expressed in dimensionless forms:

$$\Theta_{MFLS}(R', Z, \varphi, Fo, Pe) = 2\exp\left[\frac{Pe}{2}R'\cos(\varphi)\right] \left[\int_{0}^{1} f(R, Fo, Pe) dZ'\right] - \int_{-1}^{0} f(R, Fo, Pe) dZ'$$
(16)

$$f(R', Z, Fo, Pe) = \frac{1}{4R} \left[\exp\left(-\frac{Pe}{2}R\right) erfc\left(\frac{R - Pe Fo}{2\sqrt{Fo}}\right) + \exp\left(\frac{Pe}{2}R\right) erfc\left(\frac{R + Pe Fo}{2\sqrt{Fo}}\right) \right]$$
(17)

$$\Theta_{\text{MFLSs}}(R', Z, \varphi, Pe) = \exp\left[\frac{Pe}{2}R'\cos(\varphi)\right] \left[\int_{0}^{1} \frac{1}{R}\exp\left[-\frac{Pe}{2}R\right]dZ'\right] - \int_{-1}^{0} \frac{1}{R}\exp\left[-\frac{Pe}{2}R\right]dZ'$$
(18)

4. Results and discussion

4.1. Validation of the new moving finite line source model

In order to validate the new analytical approach, a comparison with a numerical simulation is needed. In the present work, the finite element code FEFLOW version 6.0 [31] is used to solve the same heat transport problem. A three-dimensional (3D) model is constructed with a horizontal domain size of $100 \text{ m} \times 200 \text{ m}$ (Fig. 1) and with 20 identical 5m layers (100 m depth). The BHE is represented by a line source for the first 50 m (top 10 layers) with an average heat flow rate of 20 W/m during 20 years of simulation. A thickness of 50 m is assigned below the BHE in order to minimize

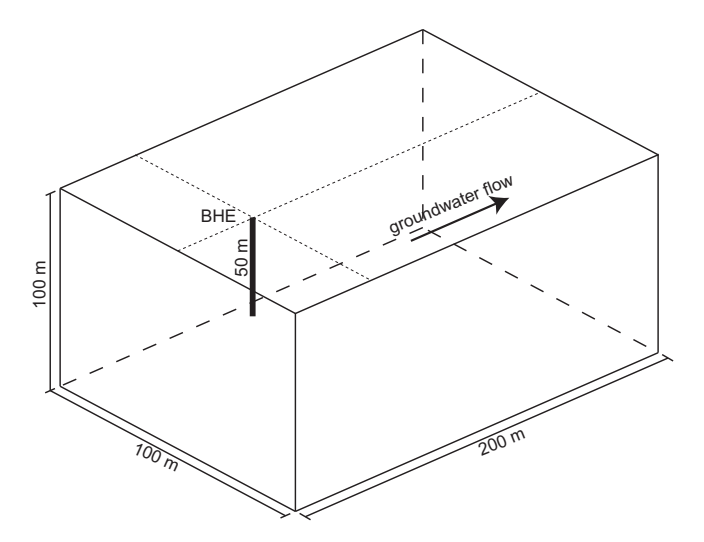


Fig. 1. 3D model used in the validation. The BHE is represented by a line source in the top $50\ m.$

boundary effects by the model bottom while still including axial effects. Fixed-head boundary conditions are applied to the left and the right model boundaries. Uniform groundwater flow is assigned throughout the aquifer. Thermal parameters of the aquifer are selected as follows: $\lambda = 2.5 \, \text{W/m/K}$, n = 0.26, $c_s = 880 \, \text{J/kg/K}$ and $\rho_s = 2650 \, \text{kg/m}^3$. The hydraulic and thermal parameters are assumed to be independent of the temperature changes. Hecht-Méndez et al. [38], for instance, stated that variable density and viscosity due to temperature changes are negligible under typical hydrogeological and operational conditions of GSHP systems.

Given that temperature changes instead of the absolute temperature are simulated, an initial temperature of $0\,^{\circ}\text{C}$ is assigned to the entire domain. Moreover, fixed ground surface temperature of $0\,^{\circ}\text{C}$ is assigned to the top layer in order to fulfil the requirements of the analytical solution.

The comparison of the analytical results with the numerical code is shown in Fig. 2. Dimensionless temperature is plotted against dimensionless distance, R', for Pe=8 and Fo=0.2 (Fig. 2a). Moreover, dimensionless temperature is also plotted against the Fourier number for two Peclet numbers, Pe=4 and Pe=8 (Fig. 2b). It can be seen in both figures that the temperature response of the analytical solution agrees with the numerical solution. Calculation of the root mean squared error yields values of 0.02 for Fig. 2a, and 0.03 for Fig. 2b. It has to be mentioned that other Peclet number scenarios as well as different space locations (x,y,z) were evaluated and also produced satisfactory results with the comparisons.

4.2. Influence of axial effects and groundwater flow on the temperature response

In order to assess the scope of the new moving finite line source model (Θ_{MFLS}), a comparison with the standard finite line source model (Θ_{FLS}) and the moving infinite line source model (Θ_{MILS}) is carried out. Note that the thermal parameters of the aquifer are set equal to the ones used in section 4.1. Fig. 3 depicts relative temperature contours (isotherms) obtained by the MFLS and MILS models in which groundwater advection is considered. Relative temperature means that the isotherms delineate a temperature difference, ΔT , between the temperature plume and ambient conditions. Note that temperature plumes are shorter for the MFLS model (Fig. 3a). Axial effects yield lower temperature changes at any given distance from the source due to the vertically dissipated

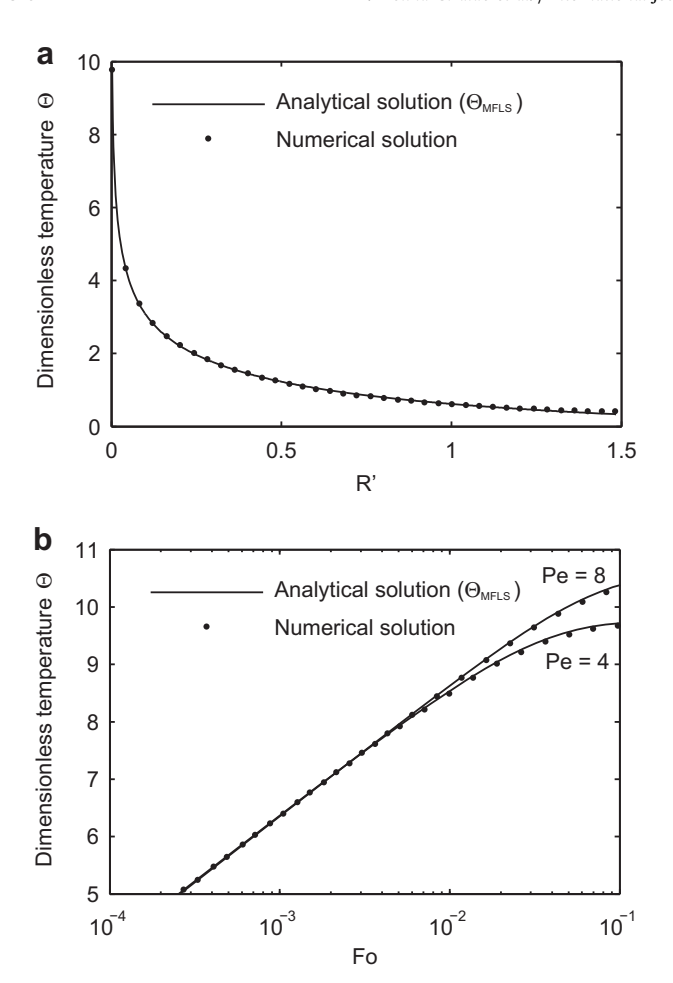


Fig. 2. Comparison of analytical (eq. (16)) and numerical results (y=0 m, z=0.5H, H=50 m): (a) temperature response (dimensionless temperature, $\Theta=4\pi\lambda\Delta T/q_{\rm L}$) over dimensionless distance R'=x/H (Fo=0.2, Pe=8); (b) temperature response over Fourier number, $Fo=at/H^2(R'=0.002)$.

heat. Therefore, neglecting axial effects could result in over-sizing of the calculated borehole lengths in designing problems for a certain energy demand [26]. Fig. 3b reveals the temperature anomaly created in the vertical direction due to the axial effects. Obviously the differences between the models are most evident close to the end points of the borehole.

Fig. 4 shows the temperature response of the MILS model (continuous black line) and the MFLS model (intermittent black lines) over a dimensionless time $(Fo/R^{\prime 2})$ for different borehole lengths. The figure clearly shows the effect of the simulation time and the borehole length on the discrepancy between the MFLS and MILS models. For longer times the discrepancy becomes more evident. Furthermore, the shorter the borehole length becomes, the earlier the time when the MFLS and MILS models start to differ and the more dominant the difference between both models. Note that the dimensionless temperature is evaluated at the center of the borehole (z = H/2), which is a common choice to approximate the temperature at the borehole wall. For steady state conditions, however, an overestimation of the temperature can occur [18,27]. Therefore, the mean temperature along the borehole length is discussed as better option for steady state conditions [18,25,27]. In the present study, for the sake of simplicity the former option is chosen.

The influence of the length of the borehole can also be seen in Fig. 5, where the temperature response is plotted over borehole

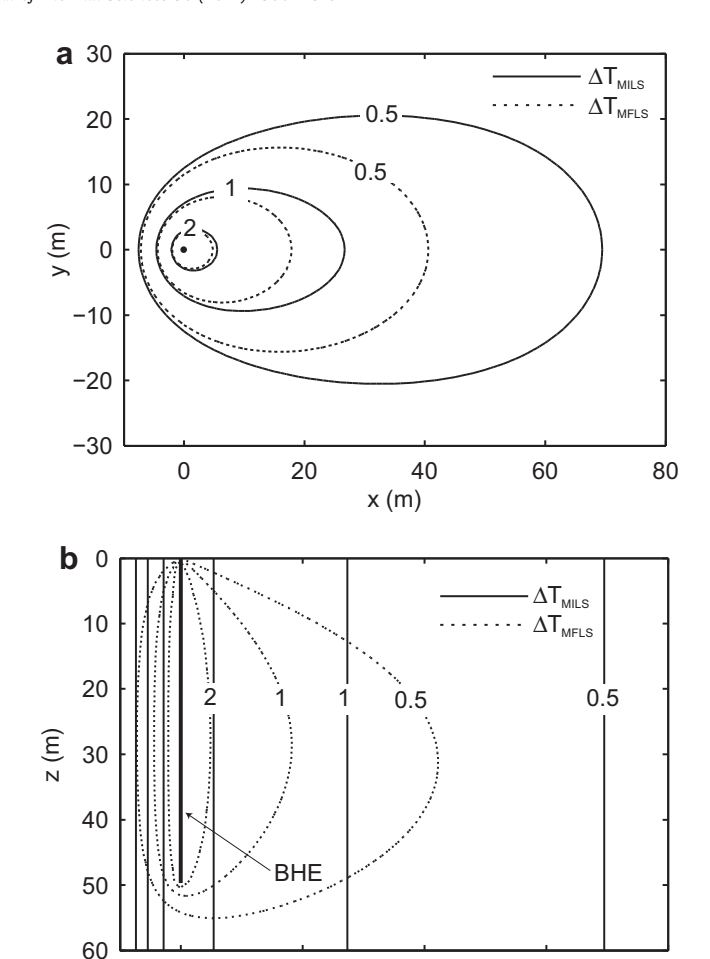


Fig. 3. Temperature change isotherms contours, ΔT (K). Dashed lines: MFLS model with H=50 m (eq. (13)); solid lines: MILS model (eq. (9)). (a) Plan view (z=0.5H); (b) vertical cross section along centerline (y=0 m). ($q_L=20$ W/m, $F_0=0.2$, $P_0=8$).

40

x (m)

60

80

20

0

lengths varying from 0 to 200 m. The shorter the borehole length is, the larger the discrepancy between the MFLS and MILS models is. For instance, for the conditions given in Fig. 5 with a Darcy velocity of 1×10^{-7} m/s, the models start to differ after around 2 years for

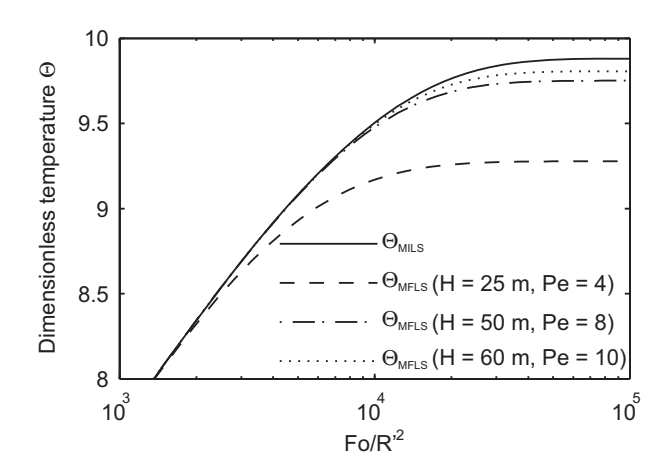


Fig. 4. Temperature response over dimensionless number $Fo/R^2 = at/x^2$ for different borehole lengths $(q = 1 \times 10^{-7} \text{ m/s}, x = 0.1 \text{ m}, y = 0 \text{ m}, z = 0.5H)$. Θ_{MILS} : moving infinite line source model (eq. (11)); Θ_{MFLS} : moving finite line source model (eq. (16)).

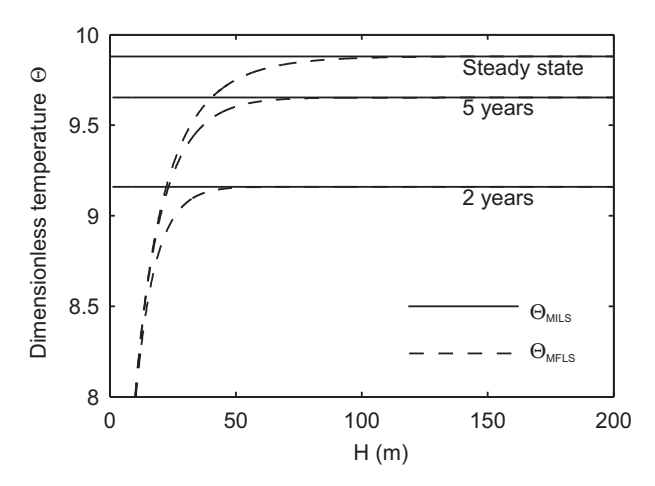


Fig. 5. Temperature response over borehole length H. $(q=1\times10^{-7} \text{ m/s}, x=0.1 \text{ m}, y=0 \text{ m}, z=0.5\text{H}, Pe=0 \text{ for } H=0 \text{ m} \text{ and } Pe=33 \text{ for } H=200 \text{ m})$. Θ_{MILS} : moving infinite line source model (eqs. (11) and (12)); Θ_{MFLS} : moving finite line source model (eqs. (16) and (18)).

boreholes with lengths shorter than 50 m. Moreover, for steady state conditions, the MILS model is valid only for a borehole length longer than 100 m.

In order to assess both the influence of groundwater flow and the axial effect, the mean temperature around a circle is evaluated for equations (6), (11) and (16). Fig. 3a shows that the temperature isotherms are not symmetrical with respect to the polar angle. Therefore, the mean temperature around a circle for the moving finite (eq. (16)) and infinite line (eq. (11)) source models can be defined as the integral average of a circle of given radius [14]:

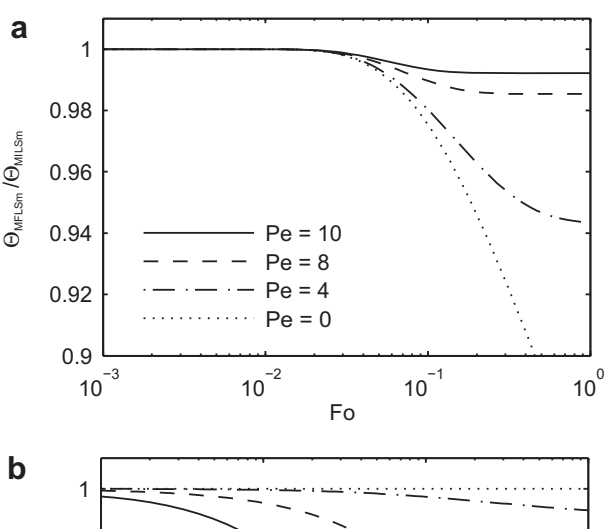
$$\Theta_{\text{MILSm}}(R', Fo, Pe) = \frac{1}{\pi} \int_{0}^{\pi} \Theta_{\text{MILS}}(R', \phi, Fo, Pe) d\phi$$
 (19)

$$\Theta_{\mathrm{MFLSm}}(R',Z,Fo,Pe) = \frac{1}{\pi} \int_{0}^{\pi} \Theta_{\mathrm{MFLS}}(R',Z,\varphi,Fo,Pe) d\varphi$$
 (20)

The ratios $\Theta_{MFLSm}/\Theta_{MILSm}$ and $\Theta_{MFLSm}/\Theta_{FLS}$ as functions of the Fourier number for different Peclet numbers are shown in Fig. 6. A decrease in these values represents an increase in the discrepancy between the MFLS and MILS model (Fig. 6a) and therefore indicates a major influence of the axial effects. Similarly, in Fig. 6b it can be seen that a decrease in the ratio corresponds to a larger discrepancy between the MFLS and FLS model (Fig. 6b) and therefore, there is a major influence of the groundwater flow.

Fig. 6a indicates that the temperature reaches the steady state condition faster at higher groundwater flow velocities. In addition, for long term simulations, the discrepancy between the models increases. This figure also reflects the effect of groundwater flow on the axial effects. It is noticeable that the larger the Peclet number the smaller the difference between the MFLS and MILS model. Hence, the axial effects are more important for low groundwater velocities. For Peclet numbers larger than 10, the discrepancy between the moving finite and the infinite solutions becomes irrelevant ($\Theta_{\text{MFLSm}}/\Theta_{\text{MILSm}} > 0.99$) at the borehole wall (x = 0.1 m). In the specific case of a borehole length of 50 m, the axial effects are negligible for Darcy velocities larger than $1.2 \times 10^{-7} \text{ m/s}$ (assuming $\lambda = 2.5 \text{ W/m/K}$). Therefore, the MILS model is still valid even for long term simulations in this groundwater flow scenario.

On the other hand, Fig. 6b shows that the discrepancy between the standard finite and moving finite line source model becomes irrelevant ($\Theta_{\text{MFLSm}}/\Theta_{\text{FLS}} > 0.99$) at the borehole wall (x = 0.1 m) for



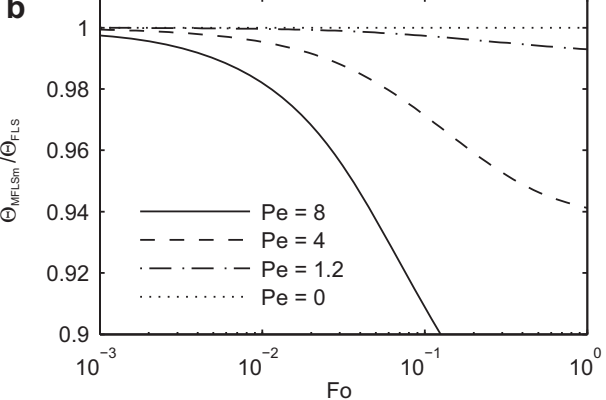


Fig. 6. Temperature response of a circle around the heat source (r = 0.1 m, H = 50 m, z = 0.5H m): (a) ratio of the MFLS and MILS model; (b) ratio of the MFLS and FLS model.

Peclet numbers lower than 1.2. Therefore, the influence of groundwater flow can be neglected in these Peclet numbers scenarios. From the aforementioned discussion, it is clear that both effects combined, axial and groundwater flow, have a major influence on the thermal response of a BHE for Peclet numbers between 1.2 and 10. It has to be mentioned that the presented results are expressed based on a Peclet number, in which the characteristic length is set to be the borehole length (H). This is to emphasize that this parameter determines the finite length of a BHE, the focus of this work. The Peclet number is a common indicator to compare the role of convection to that of conduction, but as in our study the characteristic length is defined dependent on the scale of investigation. For instance, it is set the borehole spacing [6], the borehole radius [17], and the radial distance [14]. Chiasson et al. [6] stated that advection has a significant effect on the GSHP system performance for Pe > 1. Sutton et al. [17] showed that for Pe > 0.01, the ground temperature response when advection is considered highly differs from the response with only conduction. Finally, Diao et al. [14] revealed that for Pe > 0.005 the impact of groundwater flow must be accounted for. Due to the different underlying characteristics lengths, these values, however, are not directly comparable. For the specific case of H = 50 m, when normalizing our results with respect to the aforementioned characteristic lengths, we obtain equivalent Pe = 0.11, 0.0013 and 0.002 for Chiasson et al. [6], Sutton et al. [17], and Diao et al. [14], respectively. These values are lower than ones suggested by the previous studies. However, this reflects the effect of accounting for a finite length and the criteria employed to decide whether advection or conduction is more relevant ($\Theta_{MFLSm}/\Theta_{FLS} > 0.99$). Additionally, our results reveal the effect of groundwater flow when axial effects are accounted for.

5. Conclusions

We presented a new analytical approach for the finite line source model that accounts for groundwater flow. The expression is derived for 3D and accounts for a constant surface temperature and vertical heat losses (axial effects). The influence of axial effects and groundwater flow on the temperature response of a BHE is assessed by comparing the new approach (moving finite line source model — MFLS) with existing analytical solutions such as the standard finite line source (FLS) model and moving infinite line source (MILS) model. Moreover, the new approach is also validated with a numerical code.

In general, we can conclude that both the groundwater flow and the axial heat flow have an effect on the temperature response from a borehole heat exchanger. Losses of heat downwards from the borehole bottom and fix temperature conditions at the surface result in lower temperature changes in the underground surrounding the BHE. This effect becomes more evident and therefore the discrepancy between the MFLS and MILS model increases with longer simulation time and shorter borehole lengths.

These axial effects, however, have a minor impact on the temperature response for high groundwater flow scenarios. Therefore, the discrepancy between the MFLS and MILS model decreases when increasing velocity. At the borehole wall (x = 0.1 m), axial effects can be neglected for Peclet numbers larger than 10. On the other hand, for low groundwater flow scenarios (Pe < 1.2) the effect of groundwater flow is negligible and only the axial effects play an important role.

We can conclude that the role of axial effects mainly depends on the groundwater velocity in the aquifer and the length of the borehole heat exchanger. The new proposed analytical approach (MFLS) can be applied to all groundwater flow conditions and borehole lengths. However, for Pe < 1.2 the use of the FLS model is still valid and for Pe > 10 the use of the MILS approach is acceptable. For a Peclet number range between 1.2 and 10 the use of the MFLS model is required. As an example, the temperature response of a borehole of 50 m in an aquifer with Darcy velocities of 1×10^{-8} m/s (Pe = 0.8) and 1×10^{-6} m/s (Pe = 8.4) can still be well represented by the FLS model and the MILS model, respectively. For an intermediate Darcy velocity of 1×10^{-7} m/s (Pe = 8.4), the temperature response however must be evaluated by the MFLS model.

Future work will be dedicated to evaluate the combined effect of groundwater flow, axial effects and natural geothermal gradient together with variable heat load and multiple boreholes.

Acknowledgements

The financial support for Nelson Molina-Giraldo and Ke Zhu from the International Postgraduate Studies in Water Technologies (IPS-WaT) by the Federal Ministry for Education and Research (BMBF) in Germany and by the EU FP7 ECO-GHP project for Peter Bayer is profoundly acknowledged. Furthermore, we would like to thank Selçuk Erol for his support with FEFLOW. The assistance of Margaret Hass in preparing the manuscript is gratefully acknowledged.

Appendix

An instantaneous energy extracted/injected (Q_1) at a point located at (x',y',z') produces a temperature increment given by the following Green's function [13] which satisfies the partial differential equation given by equation (1):

$$\Delta T(x,y,z,t) = \frac{Q_1}{8\rho c(\pi a t)^{3/2}} \exp\left[-\frac{(x-x')^2 + (y-y')^2 + (z-z')^2}{4at}\right]$$
(A1)

The temperature response at a given time t due to an energy extracted/injected $Qd\tau$ for a continuous point source after applying the moving source theory [13] yields the moving point source equation for a continuous injection:

$$\Delta T(x, y, z, t) = \frac{Q}{8\rho c(\pi a)^{3/2}} \int_{0}^{t} \frac{1}{(t - \tau)^{3/2}} \times \exp \left[-\frac{[x - v_{T}(t - \tau)]^{2} + (y - y')^{2} + (z - z')^{2}}{4a(t - \tau)} \right] d\tau \quad (A2)$$

Applying a change of variable, $\Psi = \frac{r}{2\sqrt{a(t-\tau)}}$, we obtain:

$$\Delta T(x, y, z, t) = \frac{Q}{2\pi^{3/2}\lambda r} \exp\left[\frac{v_{\text{T}}x}{2a}\right] \int_{r/2\sqrt{at}}^{\infty} \exp\left[-\psi^2 - \frac{v_{\text{T}}^2 r^2}{16a^2\psi^2}\right] d\psi$$
(A3)

For steady state conditions equation (A3) becomes:

$$\Delta T(x, y, z) = \frac{Q}{4\pi\lambda r} \exp\left[-\frac{\nu_{\rm T}(r-x)}{2a}\right] \tag{A4}$$

In order to account for axial effects and constant ground surface temperature conditions, the method of images [13,15] is applied to equation (A3):

$$\Delta T_3(x, y, z, t) = \frac{q_L}{2\pi\lambda} \exp\left[\frac{v_T x}{2a}\right] \left[\int_0^H f(x, y, z, t) dz' - \int_{-H}^0 f(x, y, z, t) dz' \right]$$
(A5)

where:

$$f(x,y,z,t) = \frac{1}{r\sqrt{\pi}} \int_{r/2\sqrt{at}}^{\infty} \exp\left[-\psi^2 - \frac{v_T^2 r^2}{16a^2 \psi^2}\right] d\psi$$
 (A6)

Equation (A5) is too complex to solve, therefore a change of variable ($\phi = \psi^2$) is applied in order to simplify equation (A6) as follows:

$$f(x, y, z, t) = \frac{1}{2r\sqrt{\pi}} \int_{r^2/4at}^{\infty} \frac{1}{\sqrt{\phi}} \exp\left[-\phi - \frac{v_{\rm T}^2 r^2}{16a^2 \phi}\right] d\phi$$
 (A7)

The integral of equation (A7) can be expressed as the generalized incomplete gamma function [39]:

$$f(x,y,z,t) = \frac{1}{2r\sqrt{\pi}}\Gamma\left(\frac{1}{2}, \frac{r^2}{4at}; \frac{v_{\rm T}^2r^2}{16a^2}\right)$$
(A8)

Moreover, the generalized incomplete gamma function can be expressed as a function of exponential and complementary error functions as follows [39]:

$$\begin{split} \Gamma\left(\frac{1}{2},u_{1};u_{2}\right) &= \frac{1}{2}\sqrt{\pi}\bigg[\text{exp}\left(-2\sqrt{u_{2}}\right)\text{erfc}\left(\sqrt{u_{1}}-\frac{\sqrt{u_{2}}}{\sqrt{u_{1}}}\right) \\ &+ \text{exp}\left(2\sqrt{u_{2}}\right)\text{erfc}\left(\sqrt{u_{1}}+\frac{\sqrt{u_{2}}}{\sqrt{u_{1}}}\right)\bigg] \end{split} \tag{A9}$$

Therefore, equation (A7) reduces to:

$$f(x,y,z,t) = \frac{1}{4r} \left[\exp\left(-\frac{\nu_{T}r}{2a}\right) \operatorname{erfc}\left(\frac{r-\nu_{T}t}{2\sqrt{at}}\right) + \exp\left(\frac{\nu_{T}r}{2a}\right) \operatorname{erfc}\left(\frac{r+\nu_{T}t}{2\sqrt{at}}\right) \right]$$
(A10)

For steady state conditions, the method of images applied to equation (A4) yields:

$$\Delta T_{3}(x, y, z) = \frac{q_{L}}{4\pi\lambda} \exp\left[\frac{\nu_{T}x}{2a}\right] \begin{bmatrix} \int_{0}^{H} \frac{1}{r} \exp\left[-\frac{\nu_{T}r}{2a}\right] dz' \\ -\int_{-H}^{0} \frac{1}{r} \exp\left[-\frac{\nu_{T}r}{2a}\right] dz' \end{bmatrix}$$
(A11)

References

- J.W. Lund, D.H. Freeston, T.L. Boyd, Direct application of geothermal energy: 2005 Worldwide review, Geothermics 34 (6) (2005) 691–727.
- [2] S. Hähnlein, P. Bayer, P. Blum, International legal status of the use of shallow geothermal energy, Renew. Sust. Energ. Rev. 14 (2010) 2611–2625.
- [3] P. Blum, G. Campillo, W. Münch, T. Kölbel, CO₂ savings of ground source heat pump systems – a regional analysis, Renew. Energ. 35 (1) (2010) 122–127.
- [4] D. Saner, R. Juraske, M. Kübert, P. Blum, S. Hellweg, P. Bayer, Is it only CO₂ that matters? A life cycle perspective on shallow geothermal systems, Renew. Sust. Energ. Rev. 14 (7) (2010) 1798–1813.
- [5] A. Mustafa Omer, Ground-source heat pumps systems and applications, Renew. Sust. Energ. Rev. 12 (2) (2008) 344–371.
- [6] A.D. Chiasson, S.J. Rees, J.D. Spitler, A preliminary assessment of the effects of ground water flow on closed-loop ground-source heat pump systems, ASH-RAE Trans. 106 (1) (2000) 380–393.
- [7] M. De Carli, M. Tonon, A. Zarrella, R. Zecchin, A computational capacity resistance model (CaRM) for vertical ground-coupled heat exchangers, Renew. Energ. 35 (7) (2010) 1537–1550.
- [8] E.J. Kim, J.J. Roux, G. Rusaouen, F. Kuznik, Numerical modelling of geothermal vertical heat exchangers for the short time analysis using the state model size reduction technique, Appl. Thermal Eng. 30 (6–7) (2010) 706–714.
- [9] S. Lazzari, A. Priarone, E. Zanchini, Long-term performance of BHE (borehole heat exchanger) fields with negligible groundwater movement, Energy 35 (35) (2010) 4966–4974.
- [10] C.K. Lee, H.N. Lam, Computer simulation of borehole ground heat exchangers for geothermal heat pump systems, Renew. Energ. 33 (6) (2008) 1286–1296.
- [11] R. Fan, Y. Jiang, Y. Yao, D. Shiming, Z. Ma, A study on the performance of a geothermal heat exchanger under coupled heat conduction and groundwater advection, Energy 32 (11) (2007) 2199–2209.
- [12] T.V. Bandos, Á. Montero, E. Fernández, J.L.G. Santander, J.M. Isidro, J. Pérez, P.J.F. de Córdoba, J.F. Urchueguía, Finite line-source model for borehole heat exchangers: effect of vertical temperature variations, Geothermics 38 (2) (2009) 263–270.
- [13] H.S. Carslaw, J.C. Jaeger, Conduction of Heat in Solids, second ed. Oxford University Press, New York, 1959.
- [14] N. Diao, Q. Li, Z. Fang, Heat transfer in ground heat exchangers with groundwater advection, Int. J. Thermal Sci. 43 (12) (2004) 1203—1211.
- [15] P. Eskilson, Thermal analysis of heat extraction boreholes, Ph.D. Thesis, University of Lund, Lund, Sweden, 1987.
- [16] Y. Man, H. Yang, N. Diao, J. Liu, Z. Fang, A new model and analytical solutions for borehole and pile ground heat exchangers, Int. J. Heat Mass Transfer 53 (13–14) (2010) 2593–2601.

- [17] M.G. Sutton, D.W. Nutter, R.J. Couvillion, A ground resistance for vertical borehole heat exchangers with groundwater flow, J. Energy Resour. ASME 125 (3) (2003) 183–189.
- [18] H.Y. Zeng, N.R. Diao, Z.H. Fang, A finite line-source model for boreholes in geothermal heat exchangers, Heat Transfer Asian Res. 31 (7) (2002) 558–567.
- [19] A. Michopoulos, N. Kyriakis, Predicting the fluid temperature at the exit of the vertical ground heat exchangers, Appl. Energy 86 (10) (2009) 2065–2070.
- [20] W. Yang, M. Shi, G. Liu, Z. Chen, A two-region simulation model of vertical Utube ground heat exchanger and its experimental verification, Appl. Energy 86 (10) (2009) 2005–2012.
- [21] S. Hähnlein, N. Molina-Giraldo, P. Blum, P. Bayer, P. Grathwohl, Ausbreitung von Kältefahnen im Grundwasser bei Erdwärmesonden. (Cold plumes in groundwater for ground source heat pump systems), Grundwasser 15 (2010) 123–133
- [22] G. Hellström, Ground heat storage thermal analyses of duct storage systems, I. Theory, Ph.D. Thesis, University of Lund, Sweden, 1991.
- [23] C. Yavuzturk, Modeling of vertical ground loop heat exchangers for ground source heat pump systems, PhD Thesis, Oklahoma State University, Stillwater, Oklahoma, LLS A. 1999
- [24] S. Signorelli, S. Bassetti, D. Pahud, T. Kohl, Numerical evaluation of thermal response tests, Geothermics 36 (2) (2007) 141–166.
- [25] M. Philippe, M. Bernier, D. Marchio, Validity ranges of three analytical solutions to heat transfer in the vicinity of single boreholes, Geothermics 38 (4) (2009) 407–413.
- [26] D. Marcotte, P. Pasquier, F. Sheriff, M. Bernier, The importance of axial effects for borehole design of geothermal heat-pump systems, Renew. Energ. 35 (4) (2010) 763–770.
- [27] L. Lamarche, B. Beauchamp, A new contribution to the finite line-source model for geothermal boreholes, Energy Build. 39 (2) (2007) 188–198.
- [28] D. Marcotte, P. Pasquier, Fast fluid and ground temperature computation for geothermal ground-loop heat exchanger systems, Geothermics 37 (6) (2008) 651–665.
- [29] H. Wang, C. Qi, H. Du, J. Gu, Thermal performance of borehole heat exchanger under groundwater flow: a case study from Baoding, Energy Build. 41 (12) (2009) 1368–1373.
- [30] J. Raymond, R. Therrien, L. Gosselin, R. Lefebvre, Numerical analysis of thermal response tests with a groundwater flow and heat transfer model, Renew. Energ. 36 (1) (2011) 315–324.
- [31] DHI-WASY, FEFLOW 6- User's Manual. DHI-WASY GmbH, Berlin, 2010.
- [32] H. Kupfersberger, Heat transfer modelling of the Leibnitzer Feld aquifer, Austria, Environ. Earth Sci. 59 (3) (2009) 561–571.
- [33] Y. Nam, R. Ooka, S. Hwang, Development of a numerical model to predict heat exchange rates for a ground-source heat pump system, Energy Build. 40 (12) (2008) 2133–2140.
- [34] C. Moyne, S. Didierjean, H.P. Amaral Souto, O.T. da Silveira, Thermal dispersion in porous media: one-equation model, Int. J. Heat Mass Transfer 43 (20) (2000) 3853–3867.
- [35] G. de Marsily, Quantitative Hydrogeology. Academic Press, San Diego, California, 1986.
- [36] P.A. Domenico, F.W. Schwartz, Physical and Chemical Hydrogeology, second ed. John Wiley & Sons Inc, New York, 1998.
- [37] K. Spitz, J. Moreno, A Practical Guide to Groundwater and Solute Transport Modeling, John Wiley & Sons Inc, New York, 1996.
- [38] J. Hecht-Méndez, N. Molina-Giraldo, P. Blum, P. Bayer, Evaluating MT3DMS for heat transport simulation of closed shallow geothermal systems, Ground Water 48 (5) (2010) 741–756.
- [39] M.A. Chaudhry, S.M. Zubair, Generalized incomplete gamma functions with applications, J. Comput. Appl. Math. 55 (1) (1994) 99–123.